Inorganic Chemistry

Article

pubs.acs.org/IC

Chemical Detection of Hydrogen Fluoride by the Phosphorus Congener of Cyclobutane-1,3-diyl

Yasuhiro Ueta, Koichi Mikami, and Shigekazu Ito*

Department of Applied Chemistry, Graduate School of Science and Engineering, Tokyo Institute of Technology, 2-12-1, Ookayama, Meguro, Tokyo 152-8552, Japan

Supporting Information

ABSTRACT: Heteroaryl-substituted air-tolerant 2,4-bis(2,4,6-tri-*t*-butylphenyl)-1,3-diphosphacyclobutane-2,4-diyls in the open-shell singlet state were synthesized by a sterically promoted regioselective S_NAr process. Here we demonstrate that these diyls are effective for capturing hydrogen fluoride (HF) generated by intermediary base-coordinated HF and amine-stabilized HF reagents. The hydrofluorination reaction predominantly occurred on the $\lambda^3\sigma^3$-phosphorus atoms to afford the energetically disfavored $1\lambda^5,3\lambda^5$-diphosphete. The positively charged *t*-butyl-substituted phosphorus atom trapped the fluoride anion, and the subsequent protonation was controlled by the steric effect. X-ray crystallographic analysis and an Atoms in Molecule study of the air-stable $1\lambda^5,3\lambda^5$-diphosphete bearing P−H and P−F bonds revealed that the delocalized ylidic linkages in the four-membered ring were almost identical, in contrast to the nonsymmetrically substituted 2,4-bis(2,4,6-tri-*t*-butylphenyl)-1,3-diphosphacyclobutane-2,4-diyl. Hydrofluorination efficiently induced a remarkable exchange of visible photoabsorption. The charge-transfer-type transition from highest occupied molecular orbital to lowest unoccupied molecular orbital was highly tuned, which is advantageous for the facile identification of HF. In contrast to hitherto known trapping reagents for HF based on cleavage of the H−F bond, several hydrofluorinated P-heterocycles were reconverted into the 1,3-diphosphacyclobutane-2,4-diyl by treatment with sodium hydride. However, in the hydrofluorination of the benzoyl-substituted 1,3-diphosphacyclobutane-2,4-diyl, fluorination and protonation occurred at the *t*-butyl-substituted phosphorus atom and the skeletal carbon atom, respectively, and the energetically preferable $1\lambda^5,3\lambda^3$-dihydrodiphosphete was isolated as a purple-blue crystalline compound. These findings are promising not only for the practical detection of HF but also for the development of fluorine technology based on the chemistry of phosphorus heterocycles.

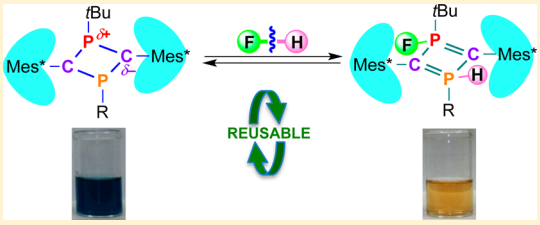

INTRODUCTION

Hydrogen fluoride (HF) is used in large quantities in industries such as the semiconductor and petroleum industries,[1] and it is the principal source of fluorine for the synthesis of many drugs and polymers.[2] However, HF is a hazardous reagent because of its low boiling point (19.5 °C) and high toxicity, and therefore an efficient method for detecting HF as well as dissociation of the H−F bond is required. Additionally, HF is the target analyte liberated in the hydrolysis of fluorinated G-type chemical warfare agents.[3,4]

A pioneering method for the chemical detection of HF uses moisture-sensitive (trifluoromethyl)dialkylaminoboranes. For example, *N*,*N*-dimethyl-1,1-bis(trifluoromethyl)boranamine (**A**) is converted into the corresponding amineborane in Et_2O in the presence of HF,[5] and the robust H−F bond (135 kcal mol^{-1})[6] of the trapped HF is cleaved. Lewis acid receptors based on boronic acids and esters have been fine-tuned over the past decades for the selective capture of fluoride anion.[7] HF is efficiently trapped in the presence of boronic acid and an appropriate base. Aldridge and co-workers reported that 2-(*N*,*N*-dimethylaminomethyl)ferrocene boronic acid (**B**; Chart 1) detected HF by formation of a ditopic complex in which HF was nearly separated into the ion pair in the dimeric structure (H−F distance in the crystalline state: 2.204 and 2.214 Å).[8]

Chart 1. Previous Compounds for Detection of HF

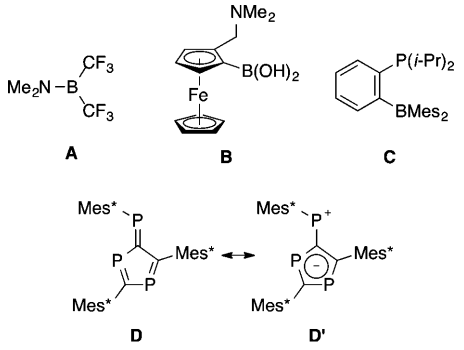

The oxidation potential of the ferrocene chromophore shifted downward upon hydrofluorination. Molecular systems related to **B**[9] were subsequently developed in which the boronic acid moiety is transformed into the BF_3 structure following removal of H_2O molecules. Substitution of boronic acid with the Mes_2B group (Mes = mesityl: 2,4,6-trimethylphenyl) resulted in the Mes groups in **C** being substituted with fluorine atoms.[10] A

Received: June 24, 2015
Published: August 27, 2015

DOI: 10.1021/acs.inorgchem.5b01399
Inorg. Chem. 2015, 54, 8778−8785

method for the facile chemical detection of HF without structural perturbation of the receptor unit is of interest, and subsequent dehydrofluorination is desirable for efficient use of the detection unit.

We speculated that the use of phosphorus compounds would provide an alternative approach for the efficient capture of HF, principally because of the large P−F bond energy (119.4 kcal mol^{-1}).[11] The kinetically stabilized 1,3,6-triphosphafulvene **D** (Mes* = 2,4,6-*t*-$Bu_3C_6H_2$)[12] successfully trapped HF and afforded a heterocyclic compound bearing the exo P(H)-ylide moiety.[13] The considerably polarized canonical structure **D′** would induce regioselective hydrofluorination, and the aromaticity of the resultant five-membered ring would facilitate construction of the P-ylide bearing a P−H bond.

We here used air-tolerant 1,3-diphosphacyclobutane-2,4-diyls of singlet biradicals (**E**; Chart 2) for the chemical detection of HF. Various air-stable biradicals **E** can be synthesized via the 1,3-diphosphacyclobuten-4-yl anion (**F**), and any suitable P-heterocyclic open-shell molecule can be synthesized.[14,15] The phosphorus atoms in **E** are positively charged due to the zwitterionic canonical formula,[16] and thus addition of the F^- species can occur regioselectively to generate the corresponding anionic intermediate.[17−19] During the course of intensive studies on the direct arylation of the 2,4-bis(2,4,6-tri-*t*-butylphenyl)-1,3-diphosphacyclobutane-2,4-diyl skeleton,[20] we found that installation of fluorinated pyrimidine substituents was useful for trapping the intermediary HF molecules and providing the $1\lambda^5,3\lambda^5$-diphosphete. The capture of HF induced remarkable changes in the physicochemical properties of $1\lambda^5,3\lambda^5$-diphosphete compared with 1,3-diphosphacyclobutane-2,4-diyl. On the basis of these findings, a series of air-tolerant P-arylated 1,3-diphosphacyclobutane-2,4-diyls were screened for HF trapping, and release of the captured HF from the hydrofluorinated P-heterocycle was subsequently investigated. Furthermore, the thermodynamically preferable structure $1\lambda^5,3\lambda^3$-dihydrodiphosphete was also realized by employing an acyl-substituted 2,4-bis(2,4,6-tri-*t*-butylphenyl)-1,3-diphosphacyclobutane-2,4-diyl. Also, structural characteristics of the $1\lambda^5,3\lambda^5$-diphosphete and $1\lambda^5,3\lambda^3$-dihydrodiphosphete were studied.

Chart 2. General Formulas of the Air-Stable 1,3-Diphosphacyclobutane-2,4-diyl and 1,3-Diphosphacyclobuten-4-yl anion

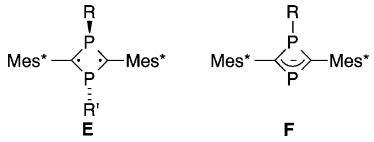

RESULTS AND DISCUSSION

Synthesis of the Pyrimidine-Substituted 1,3-Diphosphacyclobutane-2,4-diyl via the Sterically Induced S_NAr Reaction. As described in our previous report,[20] we synthesized a novel P-heteroarylated 1,3-diphosphacyclobutane-2,4-diyl via the S_NAr reaction of the 1,3-diphosphacyclobuten-4-yl anion. Reaction of phosphaalkyne **1**,[14,21] 0.5 equiv of *t*-butyllithium, and 5-chloro-2,4,6-trifluoropyrimidine[2b,22] afforded the pyrimidine-substituted **3** in 80% isolated yield via regioselective activation of the C−F bond by **2** (Scheme 1). The calculated highest occupied molecular orbital (HOMO) of

Scheme 1. Preparation of 3 via the Regioselective S_NAr Reaction of P-Heterocyclic Anion 2

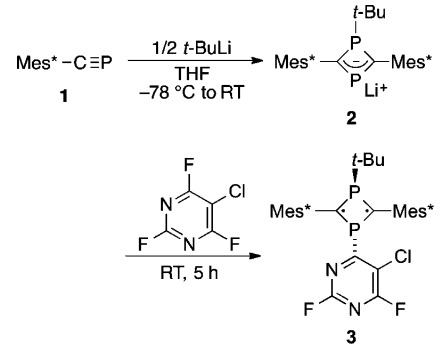

2, optimized at the CAM-B3LYP/6-31+G(d) level (Figure 1),[23] indicated that P−C bond formation is not regulated by

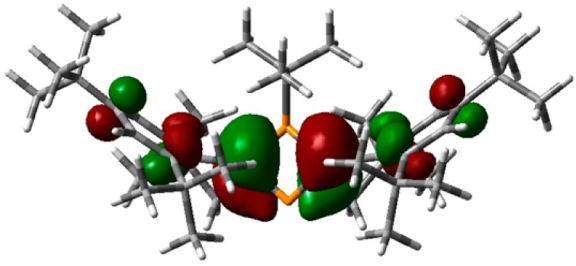

Figure 1. HOMO of **2** (without Li^+; −2.08 eV).

orbital control. Furthermore, the positively charged sp^2 phosphorus atom (Mulliken charge = +0.816) is not compatible with nucleophilic arylation as the charge-control process. Although the details remain unclear, steric effects around the heterocyclic allylic system of **2** might facilitate regioselectivity, affording products such as **3**.[24] Crystalline **3** could be handled in air, and the structure was characterized by spectroscopic measurements. ^{19}F NMR showed the presence of nonequivalent fluorine atoms (δ_F −47.2, −62.1), and the skeletal carbon atoms were observed by ^{13}C NMR at δ_C 97.8 with coupling to the ^{31}P nuclei ($^1J_{PC}$ = 35.5, 25.7 Hz). The UV−vis spectrum of **3** showed a visible absorption at 635 nm, and irreversible oxidation potentials of **3** were observed by cyclic voltammetry (see Supporting Information).

Trapping HF by the Pyrimidine-Substituted 1,3-Diphosphacyclobutane-2,4-diyl. Subsequent S_NAr reaction of **3** with lithium diethylamide was examined next. Compound **3** was reacted with 3 equiv of lithium diethylamide to afford the dually substituted product **4** in 78% yield (Scheme 2, Path A). Although **5** was generated in the reaction of **3** with 1 equiv of lithium diethylamide, **5** could not be isolated from the cogenerated products. Compound **4** was characterized spectroscopically and further studied by X-ray crystallographic analysis. This analysis was partially successful due to disorder of the *t*-butyl group (Figure S1), but the sp^2-like skeletal carbon atoms [$\sum_{angles}$ = 357.7(3), 359.9(3)°] and pyramidalized phosphorus atoms [$\sum_{angles}$ = 349.6(3), 313.4(2)°] could be unambiguously characterized. The N atoms in the diethylamino groups showed a nearly planar structure [$\sum_{angles}$ = 358.5(4), 352.8(5)°], indicating that the lone pairs of amino groups substantially conjugated with the N-heterocyclic system. The distances of the skeletal bonds (1.702−1.803 Å) are comparable to those of the P-arylated 1,3-diphosphacyclobu-

DOI: 10.1021/acs.inorgchem.5b01399
Inorg. Chem. 2015, 54, 8778−8785

Scheme 2. Subsequent S_NAr Reaction of 3 (Path A) and Capture of the Eliminated HF Molecule in the Reaction Mixture (Path B)

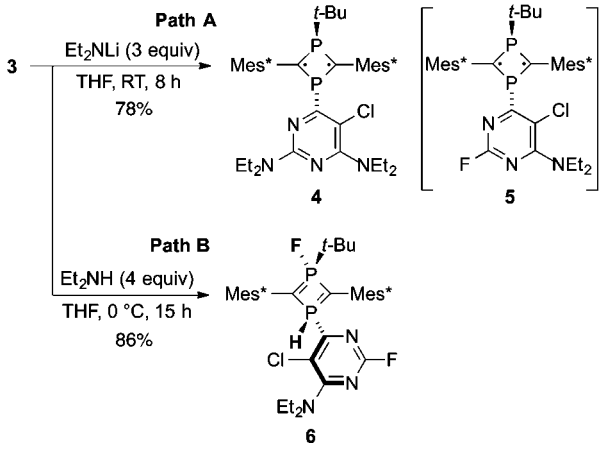

tane-2,4-diyls.[20] The cyclic voltammogram of **4** confirmed a good electron-donating capability (+0.21 V vs Ag/AgCl, see Supporting Information).[25] The S_NAr reaction of **3** with 3 equiv of sodium butoxide provided the corresponding product (50% yield, see Supporting Information).

Next, we attempted the subsequent S_NAr reaction of **3** with nonmetallic nucleophiles. In contrast to the reaction with lithium diethylamide, mixing an excess (4 equiv) of diethylamine with **3** suppressed the dual substitution of the fluorine atoms and promoted hydrofluorination of the phosphorus atoms to afford **6** as an air-stable crystalline compound in 86% yield (Scheme 2, Path B). In this reaction, the HF-amine complex $[Et_2NH{\cdot}(HF)_n]$ cogenerated via removal of the fluorine atom would strongly interact with the intermediary monosubstituted product **5**. The ^{19}F NMR spectrum of **6** showed the P−F fluorine atom at δ_F −63.4, and in the ^{13}C NMR spectrum, the ylidic carbon atoms were observed at higher field (δ_C 26.2). ^{31}P NMR showed magnetically coupled phosphorus atoms of **6** (δ_P −13.0, 79.1; $^2J_{PP}$ = 137.3 Hz) accompanying the characteristic P−H and P−F spin−spin couplings ($^1J_{PH}$ = 488.3 Hz, $^1J_{PF}$ = 1127.0 Hz). The ^1H NMR spectrum showed the P−H proton at δ_H 9.20 ($^3J_{PH}$ = 46.8 Hz), and the J_{PH} and J_{PF} data are comparable to those of the exo-hydrofluorinated product of 1,3,6-triphosphafulvene **C** ($^1J_{PH}$ = 573.6 Hz, $^1J_{PF}$ = 1077.3 Hz).[13]

Chart 3. Molecules for the Density Functional Theory Calculation

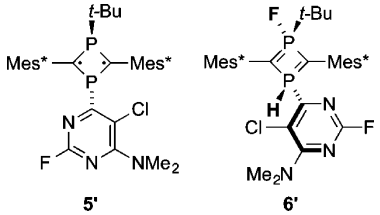

Structural and Photoabsorption Properties of the Hydrofluorinated P-Heterocycle. Figure 2 shows the molecular structure of **6**. The steric encumbrance is decisive for the trans geometry of the H−P···P−F system. The distances of the skeletal P−C bonds were nearly identical and were comparable to the P−C distances of phosphonium ylides.[26]

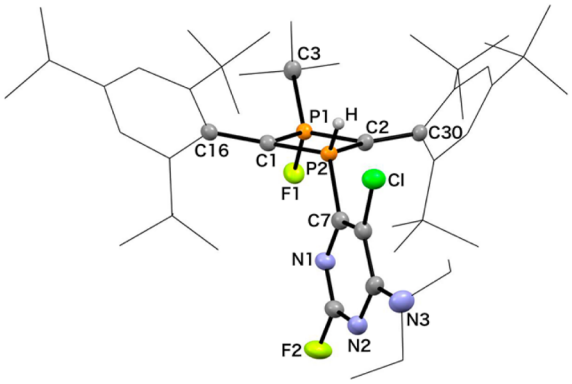

Figure 2. Molecular structure of **6** (50% probability level). Hydrogen atoms except for the P−H group and the disordered structure are omitted for clarity. Selected bond lengths (Å) and angles (deg): C1−P1 1.731(2), C2−P1 1.734(2), C1−P2 1.751(2), C2−P2 1.755(2), F1−P1 1.598(1), C3−P1 1.852(2), C7−P2 1.869(2), H−P2 1.23(2), C1−C16 1.506(2), C2−C30 1.503(2), P1−C1−P2 87.40(7), P1−C1−C16 127.2(1), P2−C1−C16 143.7(1), P1−C2−P2 87.22(7), P1−C2−C30 125.7(1), P2−C2−C30 146.2(1), C1−P1−C2 93.38(8), C1−P1−C3 120.26(8), C2−P1−C3 120.82(8), C1−P1−F1 115.21(7), C2−P1−F1 112.16(7), C3−P1−F1 96.35(7), C1−P2−C1 91.99(7), C1−P2−C7 117.59(8), C2−P2−C7 114.93(8), C2−P2−H 116.7(9), C1−P2−H 115.8(9), C7−P2−H 100.9(9), C3−P1···P2 137.50(6), C7−P2···P1 129.83(6).

Thus, the skeletal P−C linkages would be distinct from **5′** (optimized at the M06-2*X*/6-31G(d) level,[27] Chart 2, Figure S2) and the previously characterized 2,4-bis(2,4,6-tri-*t*-butylphenyl)-1,3-diphosphacyclobutane-2,4-diyls.[20] Two skeletal carbon atoms exhibited an almost planar sp^2-type structure [∑(angles) = 358.3 (C1), 359.1 (C2)]. The P_2C_2 four-membered ring requires a perpendicular-type conformation with the pyrimidine ring (τ = 88.4°), whereas the related 1-heteroaryl-1,3-diphosphacyclobutane-2,4-diyls[20] prefer π-type conjugation between the P_2C_2 ring and the aryl substituent via the lone pair of the aryl-substituted phosphorus atom. Density functional theory (DFT) calculation for **6′** (Figure S3) supported the spiro-type conjugation between the pyrimidine ring and the skeletal P−C σ^* orbital (vide infra). The Mes* aromatic rings are highly distorted into the boat-like structures[28] and are not coplanar with the four-membered $1\lambda^5,3\lambda^5$-diphosphete ring (torsion angles: 60°, 62°).

To further understand the structural characteristics of **6**, Atoms in Molecules (AIM)[29] analysis of **6′** (Chart 2) was conducted based on the data obtained at the B3LYP/6-311G(2d,p)//M06-2*X*/6-31G(d) level. Figure 3a shows the Laplacian map in the P_2C_2 plane of **6′** together with bond paths and bond critical points (BCPs). The position of each skeletal BCP is greatly shifted toward the electropositive phosphorus atoms, indicating accumulation of electron density in the basin of the electronegative carbon atoms. The bond ellipticity values at the skeletal P−C bonds of **6′** are smaller than those of the related 1,3-diphospahcyclonbutane-2,4-diyls,[20] indicating that the skeletal bonds of **6** are affected by π-delocalization and are distinct from those of the diphosphacyclobutanediyl moiety.[20] Figure 3b shows the Laplacian map of the cross section through the P_2C_2 plane. All the negative Laplacian values at the skeletal BCPs characterize the covalent bonding character, which is identical to that of phosphonium ylide.[30,31] However, the positive Laplacian for the BCP between P and F ($\nabla^2\rho$ = +0.54 e Bohr^{-5}) indicates the ionic-bond character of the P−F linkage.

DOI: 10.1021/acs.inorgchem.5b01399
Inorg. Chem. 2015, 54, 8778−8785

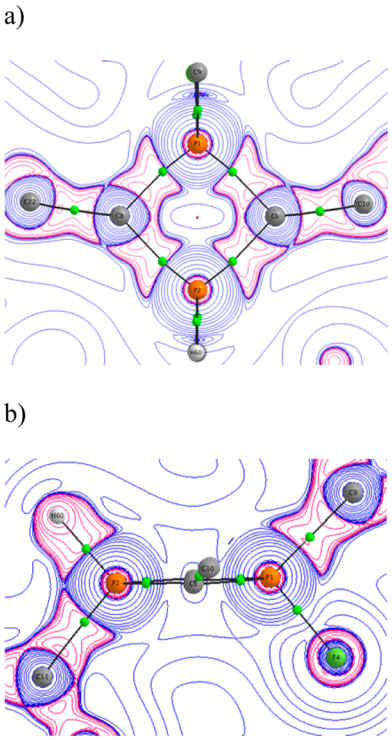

Figure 3. (a) The Laplacian map (blue: $\nabla^2\rho > 0$; red: $\nabla^2\rho < 0$) in the plane P1−C1−P2−C2 and (b) in the plane C_{Mes*}−(F)P1···P2-(C_{Mes*}H)−H of **6′** with bond paths (black lines) and bond critical points (BCPs, green dots). Contours are drawn at logarithmic intervals in $-\nabla^2\rho$/e Bohr^{-5}. $\nabla^2\rho$ at the BCPs: P1−C1 −0.34, P1−C2 −0.34, P2−C1 −0.32, P2−C2 −0.31. Bond ellipticity at the BCPs: P1−C1 0.26, P1−C2 0.26, P2−C1 0.23, P2−C2 0.23, C1−C_{Mes*} 0.10, C2−C_{Mes*} 0.09, P1−$C_{t\text{-}Bu}$ 0.04, P1−F 0.02, P2−H 0.03, P2−C_{aryl} 0.10.

Figure 4 shows the UV−vis spectrum of **6**. A weak and broad visible absorption was observed at 583 nm, together with strong

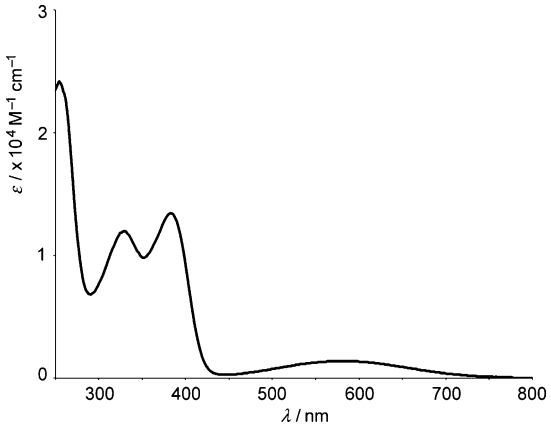

Figure 4. UV−vis spectrum of **6** in dichloromethane.

absorptions in the ultraviolet area. Time-dependent (TD) DFT calculation of **6′** [M06-2*X*/6-31G(d)] qualitatively assigned the weak visible absorption to transition from HOMO to lowest unoccupied molecular orbital (LUMO; see Supporting Information). Whereas the HOMO of **6′** mainly reflects contributions from the skeletal carbons and the Mes* aromatic rings, the LUMO mainly reflects contributions from the pyrimidine unit. Thus, the characteristics of the molecular orbitals correspond to the small absorption coefficient of the visible absorption. As indicated by the HOMO and LUMO of **6′**, the pyrimidine ring and the 1λ^5,3λ^5-diphosphete cycle show spiro-type interaction (Figure 5), and the LUMO can be

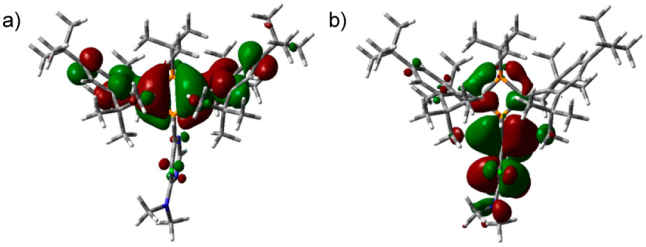

Figure 5. (a) HOMO and (b) LUMO of **6′**.

effectively tuned by the substituents on the phosphorus atoms. The visible absorption of **6** is comparable to the photoabsorption property of dichlorocarbene ylides.[32]

Density Functional Theory Study for the Regioselective Hydrofluorination. We next investigated the regioselectivity of hydrofluorination of the open-shell singlet P-heterocycle based on the DFT calculation data (Figure 6). The

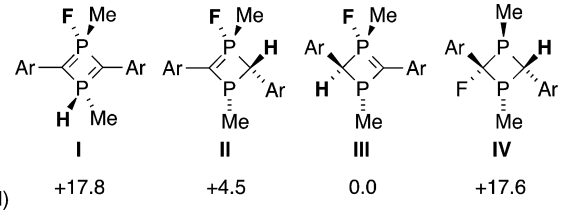

Figure 6. Relative energies of the hydrofluorinated products of 2,4-bis(2,6-di-*t*-butylphenyl)-1,3-dimethyl-1,3-diphosphacyclobutane-2,4-diyl [M06-2*X*/6-31G(d,p)]. Ar = 2,6-*t*-$Bu_2C_6H_3$.

structure of 2,4-bis(2,6-di-*t*-butylphenyl)-1,3-dimethyl-1,3-diphosphacyclobutane-2,4-diyl was used as a model to understand the stability of the 1λ^5,3λ^5-diphosphete and the corresponding isomers. The 1λ^5,3λ^5-diphosphete **I** was intrinsically unstable in comparison with the related 3-fluoro-1,2-dihydro-1λ^3,3λ^5-diphosphetes **II** and **III**, in accordance with the number of ylidic P═C bonds. However, 1,3-diphosphetane **IV** was unstable compared to **II** and **III**, indicating that steric congestion can destabilize the inherently favored structure.[17] Therefore, hydrofluorination of the intermediary **5** to afford **6** would proceed under kinetic control. Additionally, the ability of the P−F bond to stabilize the ylide structure[31] would support the formation of **6**. 3-Fluoro-1,2-dihydro-1λ^3,3λ^5-diphosphete is an unfavorable structure due to an unstable P-ylide bearing a P−H bond (see Supporting Information).

Regioselective addition of hydride anion preferentially occurs at the sterically less hindered phosphorus atom in the kinetically stabilized 1,3-diphosphacyclobutane-2,4-diyl.[17,18a] However, in the hydrofluorination reaction, the positively charged *t*-Bu-substituted phosphorus in **5** (Mulliken charge of **5′** = 0.549) would predominantly interact with the fluoride ion of HF, affording the corresponding fluorinated anionic heterocycle. As indicated by the LUMO of **5′** (Figure 7), the larger coefficient at the *t*-butyl substituted phosphorus atom would also facilitate the regioselective contact with the F atom. Thus, the interaction between the *t*-BuP moiety and the fluoride ion is explainable by both orbital and charge controls. Steric hindrance would strongly prevent interaction between

DOI: 10.1021/acs.inorgchem.5b01399
Inorg. Chem. 2015, 54, 8778−8785

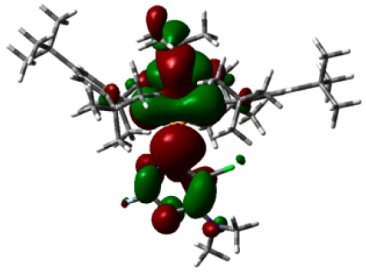

Figure 7. A plot of LUMO (#220) of **5′** (M06-2*X*/6-31G(d)).

the negatively charged skeletal carbons and the reagents, bringing about the subsequent regioselective protonation and affording **6**.

Capture and Release of HF by the Open-Shell P-Heterocycle. The successful capture of HF by the P-heterocyclic singlet open-shell system of **5** prompted us to investigate trapping HF by other 1,3-diphosphacyclobutane-2,4-diyls. Taking the putative initial interaction with the fluoride ion into account, a structure bearing a relatively electron-deficient substituent on the phosphorus atoms would be desirable for prompt capture of HF. 3HF·NEt_3 (TREAT-HF)[33−35] and in situ generated HF−amine complex from pentafluoropyridine and diethylamine were used as the source of HF.

The halogenated pyrimidine substituent of **3** facilitated the trapping of HF from 3HF·NEt_3, and **7** was isolated in 92% yield (Scheme 3). The capture of HF even using stable 3HF·NEt_3

Scheme 3. Trapping HF by the Electron-Deficient Pyrimidine-Substituted P-Heterocycle

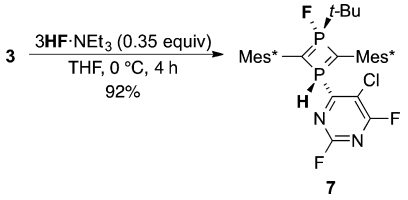

indicated a large interaction of the fluoride ion with **3** to generate the labile P-heterocyclic anion.[36] The UV−vis spectrum of **7** clearly showed that the capture of HF accompanied a remarkable red shift in the visible absorption (Table 1; see also Supporting Information). The chlorodifluoropyrimidine substituent would be effective for both the HOMO and LUMO, and the N-heteroaryl group mainly contributes to the LUMO. Therefore, the energy gap between HOMO and LUMO of **7** (see Table 2) is smaller than that of **3** due to the low-lying LUMO level of the N-heterocycle and the larger spiro-like interaction between the N-heterocycle and the P_2C_2 ring (see Figure 5). However, distinguishing between **3** and **7** by visual observation may be difficult.

We next examined the capture of HF by the triazine-substituted 1,3-diphosphacyclobutane-2,4-diyls[20] and found that the azide-substituted derivative (**8**) showed an ability comparable to **3** for trapping HF from 3HF·NEt_3 (Scheme 4, condition (i)) and afforded **9** as a green solid in 65% yield. The calculated energies of the HOMO and LUMO of **9** were almost identical to those of **8**, and correspondingly, the visible photoabsorption of **9** was almost identical to that of **8** (Tables

Table 1. λ_{max} Data (nm) of 3, 5−7, and 8−11 in Dichloromethane

R	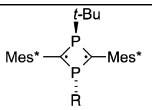	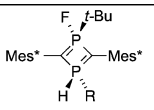
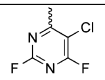	635	698
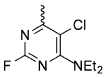	585	580
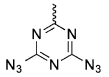	671	662
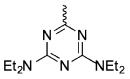	595	— [a]

[a] λ_{edge} = 594 nm.

Table 2. Molecular Orbital Properties of 3, 5′, 6′, 7, and 8−11

R	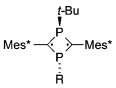		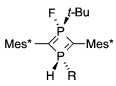	
	HOMO[a]	LUMO[a]	HOMO[a]	LUMO[a]
	−5.81	−1.19	−5.72	−1.40
	−5.59	−0.87	−5.49	−0.85
	−5.71	−1.22	−5.70	−1.25
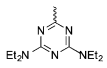	−5.35	−0.81	−5.38	−0.10

[a] In electronvolts; M06-2*X*/6-31G(d).

Scheme 4. Capture of HF by the Triazine-Substituted P-Heterocycle[a]

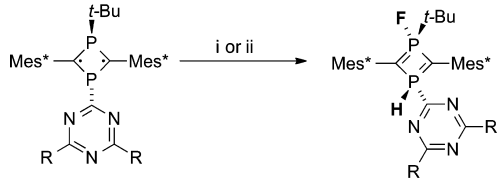

[a] Conditions: (i) 3HF·NEt_3 (0.35 equiv), 0 °C, 4 h, 65% yield (for **8**). (ii) C_5F_5N (2.0 equiv), $NHEt_2$ (4.1 equiv), room temperature, 14 h, 47% yield (for **10**).

DOI: 10.1021/acs.inorgchem.5b01399
Inorg. Chem. 2015, 54, 8778−8785

1, 2), probably due to higher LUMO level of N-heterocycle and the smaller spiro-type conjugation compared to **7**.

As indicated in Figure 5, the LUMO of the hydrofluorinated structure is composed of mainly aryl substituents on the phosphorus atom. Thus, we speculated that relatively electron-rich aryl substituents would widen the HOMO−LUMO energetic gap of the HF adduct because of the higher LUMO level of the aryl substituent. Therefore, we next examined the capture of HF by the considerably electron-donating **10**.[20] Whereas reaction of **10** and 3HF·NEt_3 yielded a trace of the hydrofluorinated product, the HF molecule generated from a mixture of pentafluoropyridine and diethylamine was successfully trapped by **10**, and **11** was isolated as a red solid in 47% yield (Scheme 4, condition (ii)). The UV−vis spectra of **9** and **11** showed highly different photoabsorption properties, suitable for visual confirmation of HF (Figure 8, Tables 1, 2; see

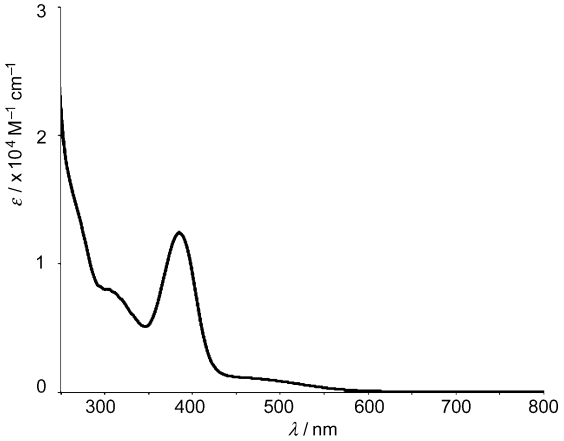

Figure 8. UV−vis spectrum of **11** in dichloromethane.

Graphical Abstract). In contrast to **6**, **7**, and **9**, the triazine ring of **11** does not show substantial spiro-type conjugation (Figure 9), probably due to the high LUMO level of the amino-substituted triazine group. Therefore, the LUMO of **11** shows a remarkably higher level compared with **6**, **7**, and **9**.

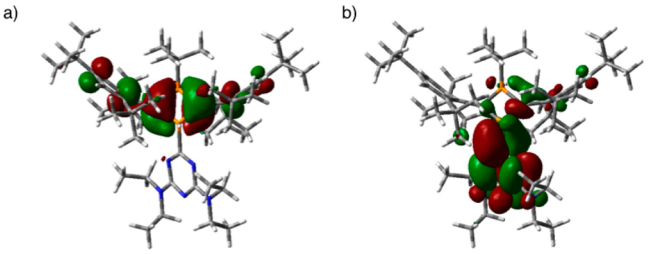

Figure 9. (a) HOMO and (b) LUMO of **11** (M06-2*X*/6-31G(d)).

We next attempted to remove the trapped HF from the hydrofluorinated P-heterocycle. The electron-deficient molecular framework of **3** and **8** would induce strong binding with HF, and treatment with base could not release HF from **7** and **9**. However, the electron-donating molecules **5** and **10** would provide relatively weak binding with HF, and thus HF bound to **11** could be removed upon treatment with sodium hydride (Scheme 5). It should be mentioned that the release of HF from **6** provides the pure monoaminated product **5**, which could not be isolated following the monoamination of **3** (see Scheme 2).

Scheme 5. Release of HF upon Treatment of Bases[a]

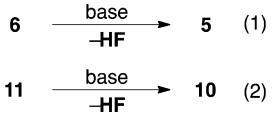

[a]Conditions: NaH (2.0 equiv), 15-crown-5 (2.0 equiv), THF, room temperature, 4 h. Yields: 74% for **5** (Eq (1)) and 72% for **10** (Eq (2)).

Formation of the Thermally Preferable $1\lambda^5,3\lambda^3$-Dihydrodiphosphete. As mentioned above, the $1\lambda^5,3\lambda^5$-diphosphete bearing both P−F and P−H bonds is the structure kinetically produced by the hydrofluorination of air-tolerant 1,3-diphosphacyclobutane-2,4-diyl. However, the thermodynamically most stable $1\lambda^5,3\lambda^3$-dihydrodiphosphete (**III** in Figure 7) can be realized by employing the benzoyl-substituted derivative **12**.[21] As described in Scheme 6, the HF generated

Scheme 6. Formation of the Thermally Preferable $1\lambda^5,3\lambda^3$-Dihydrodiphosphete

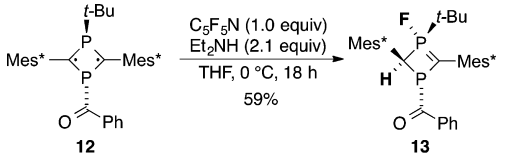

from perfluoropyridine and diethylamine was allowed to react with **12** to afford **13** in 59% isolated yield. The ^{31}P NMR spectrum of **13** indicated that the benzoyl-substituted phosphorus (δ_P = 52.0) exhibits a relatively small spin−spin coupling constant with the proton and that the *t*-butyl-substituted phosphorus is fluorinated (δ_P = 56.1, $^1J_{PF}$ = 1249 Hz, $^3J_{PF}$ = 77 Hz). The $^2J_{PP}$ constant of **13** (31.6 Hz) is smaller than that of the $1\lambda^5,3\lambda^5$-diphosphete system. The ^{19}F NMR spectrum showed a resonance accompanying spin−spin coupling with the skeletal phosphorus atoms at δ_F = −31.1, which is lower than that observed with $1\lambda^5,3\lambda^5$-diphosphetes. Although the reaction mechanism has not been verified, it is plausible that the intermediary $1\lambda^5,3\lambda^5$-diphosphete is protonated,[13] and subsequently the P−H proton is removed.

The structure of purple-blue crystalline **13** was analyzed by X-ray crystallography (Figure S4). The quality of structure optimization was poor due to disorder,[37] but the structure of the four-membered ring skeleton containing the cis-positioned F and H atoms was determined. The DFT-optimized structure of **13** is nearly identical to the X-ray structure (Figure 10). The ylidic P═C distance [X-ray: 1.658(5) Å] is comparable to that of $Ph_3P{=}CH_2$,[26d] in sharp contrast to the skeletal P−C bonds of **6**. The C2 atom shows a weakly sp^3-hybridized structure ($\sum$ = 341° except for the H atom). AIM analysis of **13** (Figure 11) indicates a substantial ellipticity of 0.41 for the polar P1−C1 bond, which is larger than the corresponding values for **6′**.[30,31] The positive $\nabla^2\rho$ value of the P−F bond (+0.47) of **13** is close to that of **6′**.

UV−vis spectrum of **13** shows a weak visible absorption (522 nm, Figure 12) and was assigned to a transition from HOMO to LUMO according to the TD-DFT calculation (see Supporting Information). The visible absorption of **13** is remarkably blue-shifted compared with that of **12** (664 nm).[21] The π-system of the ylidic P═C bond and the sp^3-phosphorus atom contribute to the HOMO, whereas the LUMO is largely constructed by the benzoyl group. Therefore, the visible

DOI: 10.1021/acs.inorgchem.5b01399
Inorg. Chem. 2015, 54, 8778−8785

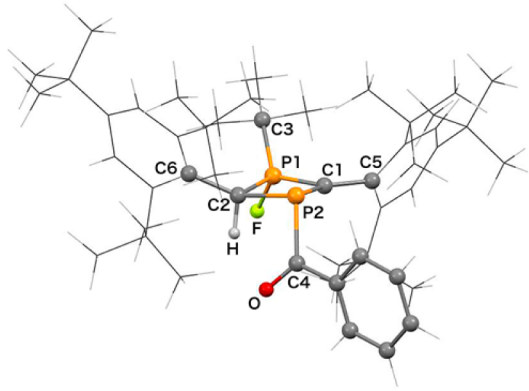

Figure 10. DFT-optimized structure of **13** [M06-2*X*/6-31G(d)]. Bond lengths (Å) and angles (deg): P1−C1 1.677, P1−C2 1.825, P2−C1 1.846, P2−C2 1.923, P1−F 1.640, P1−C3 1.856, P2−C4 1.926, C4−O 1.216, C1−C5 1.495, C2−C6 1.530, C1−P1−C2 92.6, C1−P1−C3 121.3, C2−P1−C3 123.8, C1−P1−F 119.7, C2−P1−C3 104.8, C3−P1−F 95.6, C1−P2−C2 84.4, C1−P2−C4 106.5, C2−P2−C4 95.8, P1−C1−P2 94.3, P1−C1−C5 123.7, P2−C1−C5 141.7, P1−C2−P2 87.2, P1−C2−C6 118.4, P2−C2−C6 135.1.

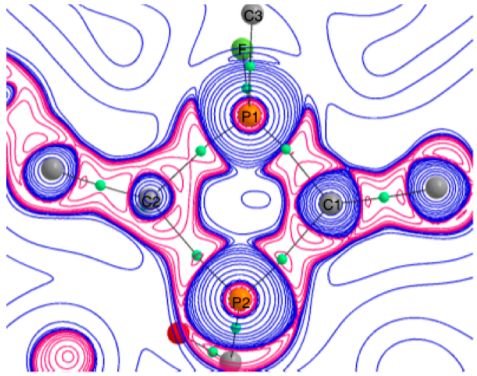

Figure 11. Laplacian map (blue: $\nabla^2\rho > 0$; red: $\nabla^2\rho < 0$) in the plane P1−C1−P2 of **13** with bond paths (black lines) and bond critical points (green dots). Contours are drawn at logarithmic intervals in $-\nabla^2\rho$/e Bohr^{-5}. $\nabla^2\rho$ at the BCPs: P1−C1 −0.22, P1−C2 −0.35, P2−C1 −0.24, P2−C2 −0.21, P1−F +0.47, P1−C3 −0.33, P2−C4 −0.24, C2−H −0.94, C4−O −0.41. Bond ellipticity at the BCPs: P1−C1 0.41, P1−C2 0.05, P2−C1 0.18, P2−C2 0.05.

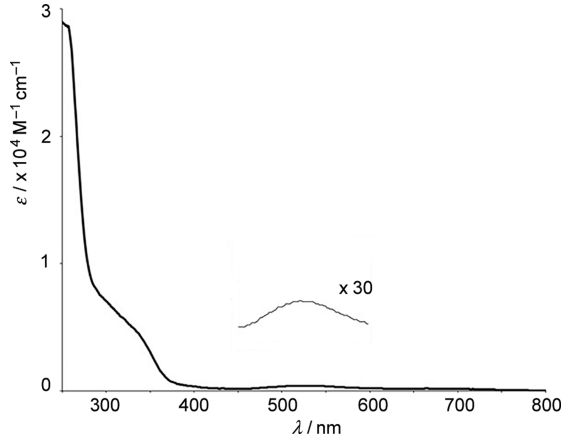

Figure 12. UV−vis spectrum of **13** in dichloromethane.

absorption of **13** is characteristic of a charge-transfer transition, which corresponds to the small absorption coefficient (Figure 13). Note that a four-membered ring containing the P-ylidic bond can be utilized as an electron-donating unit and can be

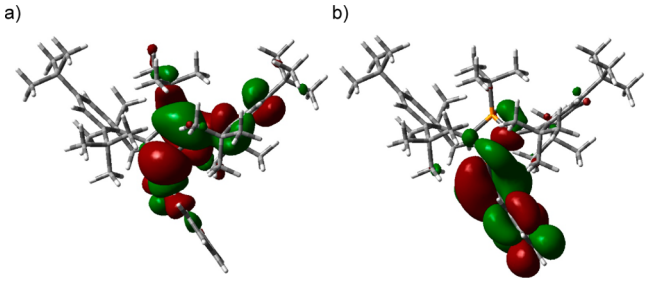

Figure 13. (a) HOMO and (b) LUMO of of **13** (M06-2*X*/6-31G(d)).

combined with any electron-accepting chromophore for inducing desirable physicochemical properties.

CONCLUSION

We have demonstrated that the air-stable singlet biradical, 1-heteroaryl-3-*t*-butyl-2,4-bis(2,4,6-tri-*t*-butylphenyl)-1,3-diphosphacyclobutane-2,4-diyl, can be utilized for capture of HF. The highly polarized skeletal P−C bonding captured both fluoride ion and proton efficiently, and the four-membered ring remained unperturbed during hydrofluorination. The heteroaryl substituent on the skeletal phosphorus atom played a decisive role in promoting both HF trapping and the stability of the hydrofluorinated P-heterocyclic skeleton. The N-heteroaryl substituent was responsible for the remarkable change in the visible photoabsorption of the charge-transfer transition upon the attachment and release of HF. Chemical modification of the hydrofluorinated P-heterocycle will provide a number of intriguing molecular structures for applications based on the chemistry of hydrogen fluoride.

Furthermore, hydrofluorination of the open-shell singlet P-heterocyclic system is attractive from the viewpoint of fundamental molecular science. As mentioned in the text, the $1\lambda^5,3\lambda^5$-diphosphete structure is mostly unstable. However, the benzoyl-substituted open-shell singlet P-heterocycle provided the most energetically favorable $1\lambda^5,3\lambda^3$-dihydrodiphosphete. The observed changes in regioselectivity likely relate to the characteristics of the open-shell singlet P-heterocycle, and attempts to elucidate the mechanism of hydrofluorination are in progress.

ASSOCIATED CONTENT

Supporting Information

The Supporting Information is available free of charge on the ACS Publications website at DOI: 10.1021/acs.inorgchem.5b01399.

Preparation of compounds, cyclic voltammograms, UV−vis spectra, crystallographic analysis, DFT calculation, and copies of NMR charts. (PDF)
X-ray crystallographic information for **4**. (CIF)
X-ray crystallographic information for **6**. (CIF)
X-ray crystallographic information for **13**. (CIF)

AUTHOR INFORMATION

Corresponding Author

*E-mail: ito.s.ao@m.titech.ac.jp.

DOI: 10.1021/acs.inorgchem.5b01399
Inorg. Chem. 2015, 54, 8778−8785

Author Contributions

The manuscript was written through contributions of all authors.

Notes

The authors declare no competing financial interest.

■ ACKNOWLEDGMENTS

This work was supported in part by Grants-in-Aid for Scientific Research (Nos. 23655173, 25105198, 25288033, and 15H00923) from the Ministry of Education, Culture, Sports, Science and Technology, Japan, the Collaborative Research Program of Institute for Chemical Research, Kyoto University (Grant Nos. 2014-09 and 2015-23), and Nissan Chemicals Co. Ltd. The authors thank Prof. Dr. T. Takao and Prof. Dr. M. Oishi of Tokyo Institute of Technology for supports of X-ray crystallographic analyses. T. T. T. Ngo supported the studies on P-heterocyclic anion **2**.

■ REFERENCES

(1) Aigueperse, J.; Mollard, P.; Devilliers, D.; Chemla, M.; Faron, R.; Romano, R.; Cuer, J. P. Fluorine Compounds, Inorganic. In *Ullmann's Encyclopedia of Industrial Chemistry;* Wiley: Weinheim, Germany, 2005.

(2) (a) Kirsch, P. *Modern Fluoroorganic Chemistry−Synthesis, Reactivity, and Applications;* Wiley: Weinheim, Germany, 2013. (b) Chambers, R. D. Fluorine in Organic Chemistry; Blackwell Publishing Ltd./CRC Press: Boca Raton, FL, 2004. (c) Hiyama, T. *Organofluorine Compounds: Chemistry and Applications;* Springer: Berlin, Germany, 2000. (d) Uneyama, K. *Organofluorine Chemistry;* Blackwell: Oxford, U.K., 2006. (e) Yoneda, N. *Tetrahedron* **1991**, *47*, 5329−5365.

(3) Sohn, H.; Létant, S.; Sailor, M. J.; Trogler, W. C. *J. Am. Chem. Soc.* **2000**, *122*, 5399−5400. See also: Létant, S. E.; Sailor, M. J. *Adv. Mater.* **2000**, *12*, 355−359.

(4) Zhang, S.-W.; Swager, T. *J. Am. Chem. Soc.* **2003**, *125*, 3420−3421.

(5) Brauer, D. J.; Bürger, H.; Pawelke, G.; Weuter, W.; Wilke, J. *J. Organomet. Chem.* **1987**, *329*, 293−304.

(6) Jacobs, T. A.; Giedt, R. R.; Cohen, N. *J. Chem. Phys.* **1965**, *43*, 3688.

(7) Nishiyabu, R.; Kubo, Y.; James, T. D.; Fossey, J. S. *Chem. Commun.* **2011**, *47*, 1106−1123.

(8) Bresner, C.; Aldridge, S.; Fallis, I. A.; Jones, C.; Ooi, L.-L. *Angew. Chem., Int. Ed.* **2005**, *44*, 3606−3609.

(9) (a) Coghlan, S. W.; Giles, R. L.; Howard, J. A. K.; Patrick, L. G. F.; Probert, M. R.; Smith, G. E.; Whiting, A. *J. Organomet. Chem.* **2005**, *690*, 4784−4793. (b) Batsanov, A. S.; Hérault, D.; Howard, J. A. K.; Patrick, L. G. F.; Probert, M. R.; Whiting, A. *Organometallics* **2007**, *26*, 2414−2419.

(10) Moebs-Sanchez, S.; Saffon, N.; Bouhadir, G.; Maron, L.; Bourissou, D. *Dalton Trans.* **2010**, *39*, 4417−4420.

(11) Finch, A. *Recl. Trav. Chim. Pays-Bas* **1965**, *84*, 424−428.

(12) Ito, S.; Sugiyama, H.; Yoshifuji, M. *Angew. Chem., Int. Ed.* **2000**, *39*, 2781−2783.

(13) Ito, S.; Miyake, H.; Yoshifuji, M.; Höltzl, T.; Veszprémi, T. *Chem. - Eur. J.* **2005**, *11*, 5960−5965.

(14) Sugiyama, H.; Ito, S.; Yoshifuji, M. *Angew. Chem., Int. Ed.* **2003**, *42*, 3802.

(15) Ito, S.; Kikuchi, M.; Sugiyama, H.; Yoshifuji, M. *J. Organomet. Chem.* **2007**, *692*, 2761−2767.

(16) Niecke, E.; Fuchs, A.; Baumeister, F.; Nieger, M.; Schoeller, W. W. *Angew. Chem., Int. Ed. Engl.* **1995**, *34*, 555−557.

(17) Ito, S.; Miura, J.; Morita, N.; Yoshifuji, M.; Arduengo, A. J., III *Inorg. Chem.* **2009**, *48*, 8063−8065.

(18) (a) Ito, S.; Miura, J.; Morita, N.; Yoshifuji, M.; Arduengo, A. J., III *Dalton Trans.* **2010**, *39*, 8281−8287. (b) Ito, S.; Ngo, T. T. T.; Mikami, K. *Chem. - Asian J.* **2013**, *8*, 1976−1980.

(19) Fuks, G.; Saffon, N.; Maron, L.; Bertrand, G.; Bourissou, D. *J. Am. Chem. Soc.* **2009**, *131*, 13681−13689.

(20) Ito, S.; Ueta, Y.; Ngo, T. T. T.; Kobayashi, M.; Hashizume, D.; Nishida, J.-i.; Yamashita, Y.; Mikami, K. *J. Am. Chem. Soc.* **2013**, *135*, 17610−17616.

(21) Sugiyama, H.; Ito, S.; Yoshifuji, M. *Chem. - Eur. J.* **2004**, *10*, 2700−2706.

(22) Parks, E. L.; Sandford, G.; Christopher, J. A.; Miller, D. D. *Beilstein J. Org. Chem.* **2008**, DOI: 10.3762/bjoc.4.22.

(23) CAM-B3LYP: Yanai, T.; Tew, D. P.; Handy, N. C. *Chem. Phys. Lett.* **2004**, *393*, 51−57.

(24) HOMO-1 of **2** [−3.33 eV, M06-2X/6-31G(d)] has significant amplitude at lone pair of the sp^2 phosphorus atom.

(25) A drop-cast fabricated semiconductor device using **4** did not show any obvious FET response, indicating small intermolecular interaction (see Figure S1).

(26) (a) Yufit, D. S.; Howard, J. A. K.; Davidson, M. D. *J. Chem. Soc. Perkin Trans. 2* **2000**, 249−253. (b) Schmidbaur, H.; Jeong, J.; Schier, A.; Graf, D.; Wilkinson, D. L.; Muller, G. *New J. Chem.* **1989**, *13*, 341−352. (c) Gilheany, D. G. *Chem. Rev.* **1994**, *94*, 1339−1374. (d) Bart, J. C. *J. Chem. Soc. B* **1969**, 350.

(27) M06-2X: Zhao, Y.; Truhlar, D. G. *Theor. Chem. Acc.* **2008**, *120*, 215−241.

(28) Ito, S.; Nanko, M.; Mikami, K. *Heteroat. Chem.* **2014**, *25*, 422−427. See also: Yoshifuji, M.; Shima, I.; Inamoto, N.; Aoyama, T. *Tetrahedron Lett.* **1981**, *22*, 3057−3060.

(29) Bader, R. F. W. *Atoms in Molecules: A Quantum Theory;* Oxford University Press: Oxford, U.K., 1990.

(30) Dobado, J. A.; Martínez-García, H.; Molina, J. M.; Sundberg, M. R. *J. Am. Chem. Soc.* **2000**, *122*, 1144−1149.

(31) Sánchez-González, A.; Martínez-García, H.; Melchor, S.; Dobado, J. A. *J. Phys. Chem. A* **2004**, *108*, 9188−9195.

(32) Moss, R. A.; Tian, J.; Sauers, R. R.; Ess, D. H.; Houk, K. N.; Krogh-Jespersen, K. *J. Am. Chem. Soc.* **2007**, *129*, 5167−5174.

(33) (a) Akana, J. A.; Bhattacharyya, K. X.; Müller, P.; Sadighi, J. P. *J. Am. Chem. Soc.* **2007**, *129*, 7736−7737. (b) Gorske, B. C.; Mbofana, C. T.; Miller, S. T. *Org. Lett.* **2009**, *11*, 4318−4321.

(34) (a) Michel, D.; Schlosser, M. *Synthesis* **1996**, 1007−1011. (b) Suga, H.; Hamatani, T.; Guggisberg, Y.; Schlosser, M. *Tetrahedron* **1990**, *46*, 4255−4260.

(35) (a) Haufe, G.; Alvernhe, G.; Anker, D.; Laurent, A.; Saluzzo, C. *J. Org. Chem.* **1992**, *57*, 714−719. (b) Bruns, S.; Haufe, G. *J. Fluorine Chem.* **2000**, *104*, 247−254.

(36) Observation of the fluorinated anionic adduct from **3** or other 1,3-diphosphacyclobutane-2,4-diyls was unsuccessful.

(37) Optimization of the structure indicated that the benzoyl-substituted phosphorus atom (P2) was partially oxidized (occupancy factor = 0.32). The oxidized compound was not observed in the course of isolation and spectroscopic measurements.

DOI: 10.1021/acs.inorgchem.5b01399
Inorg. Chem. 2015, 54, 8778−8785